Current Applied Physics 51 (2023) 22–28

Contents lists available at ScienceDirect

Current Applied Physics

journal homepage: www.elsevier.com/locate/cap

Multidimensional structural coloration from hierarchically designed plasmonic structures

Yun-jo Lee [a], Jae Seon Yu [a], Young-Seok Kim [b], Young Min Song [c,**], Sun-Kyung Kim [a,*]

[a] Department of Applied Physics, Kyung Hee University, Gyeonggi-do, 17104, Republic of Korea
[b] Display Research Center, Korea Electronics Technology Institute, Gyeonggi-do, 13509, Republic of Korea
[c] School of Electrical Engineering and Computer Science, Gwangju Institute of Science and Technology, Gwangju, 61005, Republic of Korea

ARTICLE INFO

Keywords:
Nanophotonics
Structural coloration
Hierarchical structure
Mode anticrossing
Surface plasmon polariton
Cavity mode

ABSTRACT

We propose a photonic strategy for multidimensional structural coloration that responds to varying illumination conditions. Both theoretical and experimental results verified that the combination of a metal/dielectric/metal cavity with a one-dimensional (1D) metal grating can increase the degree of freedom of structural coloration. We fabricated Ag/MgF_2/Ag cavities coupled to 1D Ag gratings (pitches of 400, 570, and 800 nm) and obtained their photonic band dispersions (i.e., angle-resolved reflectance spectra) to unravel their mode characteristics. The 1D Ag grating and Ag/MgF_2/Ag cavity induced surface plasmon polariton (SPP) and Fabry–Perot cavity modes, respectively. Notably, only a cavity mode emerged in the *s*-polarization and gradually blueshifted with increasing angle, whereas in the *p*-polarization, both SPP and cavity modes appeared and shifted oppositely with changes in the angle, leading to intricate color patterns at different wavelengths, angles, and polarizations. To further understand the effect of each mode upon structural coloration, we obtained the distribution of electric field intensity using rigorous coupled-wave analysis simulation, which identified multiple photonic bands in the *p*-polarization as various SPP-mediated hybrid modes.

1. Introduction

Colors are optical properties that describe how an object interacts with visible light, and they are ubiquitous in our daily surroundings. Conventional methods for displaying colors involve the use of pigments and dyes, which are applied to surfaces and fabrics. However, these techniques have environmental drawbacks and tend to fade over time [1–3]. To address these concerns, researchers have turned to structural coloration. Unlike pigment or dye-based coloration, structural coloration does not undergo chemical reactions and is resistant to fading unless the underlying structure is mechanically disrupted [4–6]. Moreover, the interaction of light with micro- and nanoscale photonic structures, such as plasmonic gratings [3,7,8], multilayers [2,9], and scattering particles [6,10,11], can create high-purity iridescent colors by either transmitting or reflecting visible light at specific wavelengths. A significant advantage of structural coloration is that the color spectrum can be readily modulated by adjusting the morphological parameters and illumination conditions. As a result, structural coloration has found applications beyond color representation, including color filters [7,9], holographic displays [12,13], optical data storage [14], and anti-counterfeiting patterns [3,15,16].

The pursuit of structural coloration through the use of plasmonic gratings, multilayers, and scattering particles has been the subject of extensive photonics research. Of these methods, plasmonic gratings have garnered considerable interest for their potential as tunable color filters. For instance, Zeng et al. demonstrated the feasibility of employing thin Ag grating-based transmissive color filters, which modulate the transmission spectrum by regulating the grating pitch [7]. It is worth noting that the spectra of plasmonic gratings should be polarization-dependent when designed one-dimensionally (1D) [8,17,18]; however, the color representation nearly vanishes in the *s*-polarization. In contrast, multilayers create structural coloration via Fabry–Perot resonances as light passes through different material layers [19–22]. The color characteristics of multilayers are determined by modulating the optical dispersions and thicknesses of the constituent materials. Li et al. designed symmetric Ag/SiO_2/Ag metal/-dielectric/metal (MDM) cavities on quartz substrates, which enabled high transmittance peaks at specific wavelengths [9]. Meanwhile, Kim

* Corresponding author. Department of Applied Physics Kyung Hee University, Gyeonggi-do, 17104, Republic of Korea.
** Corresponding author. School of Electrical Engineering and Computer Science Gwangju Institute of Science and Technology, Gwangju, 61005, Republic of Korea.
E-mail addresses: ymsong@gist.ac.kr (Y.M. Song), sunkim@khu.ac.kr (S.-K. Kim).

https://doi.org/10.1016/j.cap.2023.04.016
Received 22 February 2023; Received in revised form 27 March 2023; Accepted 18 April 2023
Available online 23 April 2023

et al. fabricated asymmetric Ag/SiO_2/Sn cavities on Si substrates, which induced wavelength-dependent absorption [1]. Both studies utilized tunable Fabry-Perot resonances by regulating the thickness of the intermediate dielectric layer and exhibited dramatic angle-dependent structural coloration. The phase difference of light with respect to the angle of incidence allows for distinct colors depending on the viewing angle. Since the morphology of multilayers is symmetric with respect to the plane, they generate polarization-independent colors. Scattering, which occurs when light interacts with particles or voids in the background, is also a viable means of producing colors [11,23,24]. Regularly arranged scattering particles (i.e., bottom-up, three-dimensional photonic crystals) provide a cost-effective approach to achieving structural coloration that is sensitive to the viewing angle. Lee et al. demonstrated the effectiveness of using colloidal nanoparticles for structural coloration, with the spectra changing depending on the diameter of the constituent nanoparticles [25].

Despite the success of previous research on structural coloration, it was limited to a single illumination condition, either polarization or incident/viewing angle. In this study, we propose hierarchically designed optical structures that integrate 1D Ag gratings with Ag/MgF_2/Ag cavities to represent a wide color gamut that is dependent on both polarization and angle. In experiments, we obtained the polarization-resolved photonic bands of the fabricated structures to understand the origin of multidimensional structural coloration. In addition, we identified the measured photonic bands by performing rigorous coupled-wave analysis (RCWA) simulations. Our study provides a comprehensive approach to achieving multidimensional structural coloration, which promises applications in optical devices and displays [3,15,16].

2. Results and discussion

2.1. Polarization and angle dependent structural coloration

The goal of this study is to investigate the optical phenomenon of structural coloration, where the color of an object arises not from pigments, but rather from the interaction of light with the physical morphology of the object. To this end, we designed a 1D metal grating-coupled MDM cavity, which is capable of switching colors depending on polarization and angle, as illustrated in Fig. 1(a). First, an Ag/MgF_2/Ag cavity was employed to create angle-dependent colors. The MDM cavity comprised top and bottom Ag layers with thicknesses of 20 and 150 nm, respectively. Upon illumination, a portion of the incident light is reflected at the top Ag surface, while the remainder is transmitted into the cavity. The reflected light from the bottom Ag surface then interferes with all partially reflected light, leading to optical resonances (i.e., reflection dips) [3,26]; their wavelengths are determined by the thickness of the MgF_2 layer, and the phase delay of light reflected at both Ag surfaces. By varying the thickness of the MgF_2 layer between 70 and 235 nm, we observed a redshift and sweep of the entire visible spectrum in the minimum of the cavity reflectance. For our structures, the thickness of the MgF_2 layer was fixed at 165 nm to achieve a pronounced reflection dip at a red wavelength for normal incidence. Note that the cavity mode blueshifts with increasing angle.

To generate polarization-induced color shifts, a 1D Ag grating was added to the MDM cavity. The Drude theory suggests that the surface plasmon polariton (SPP) resonance wavelength (λ_p) of a metal grating depends on its pitch (P) and width (w) such that $\lambda_p = \sqrt{\pi^2 Pw}$, leading to a redshift in resonance wavelength with an increase in pitch and width for one specific polarization [18,27,28]. As a result, the combination of the Ag/MgF_2/Ag cavity and 1D Ag grating structures allows for the observation of structural coloration that is reliant on both polarization and angle. Fig. 1(b) depicts the resulting coloration depending on angle and polarization when the Ag grating pitch is 400, 570, or 800 nm. The hybrid resonances via the cavity and grating enable the creation of a wide range of color variations that depend on various structural parameters [29–31]. To induce substantial coupling between the cavity mode and SPP mode, the thickness of the top Ag layer in the MDM cavity was fixed at 20 nm, which is comparable to a skin depth of Ag. In addition, a grating pitch of 400 nm was found to be adequate in terms of color variation, as it can excite diverse hybrid plasmonic modes, which

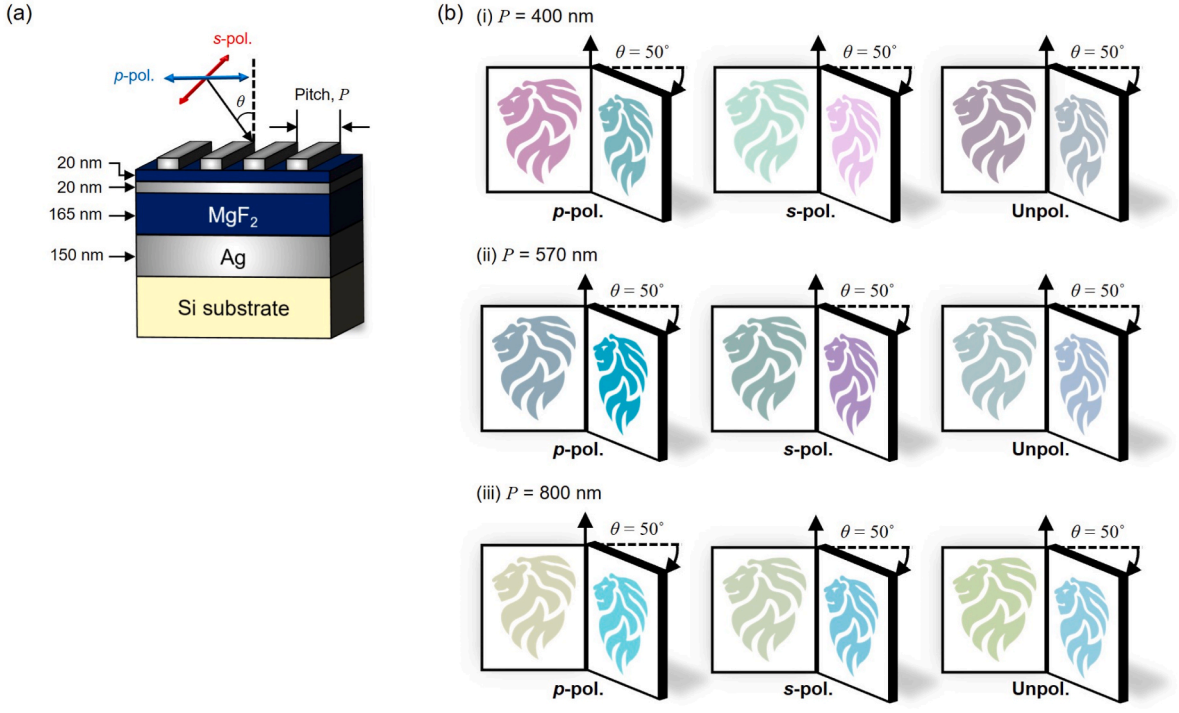

Fig. 1. (a) Schematic of a proposed plasmonic grating coupled metal/dielectric/metal (MDM) cavity. (b) Predicted color images of the proposed structures with different P values (400, 570, 800 nm) for p-, s-, and unpolarized light when the angle of incidence is 0° or 50°. Each color is obtained based on the measured spectra in Fig. 3a–c. (For interpretation of the references to color in this figure legend, the reader is referred to the Web version of this article.)

will be discussed in detail in Fig. 5.

2.2. Fabrication of 1D Ag grating coupled Ag/MgF_2/Ag cavity

We fabricated a 1D grating-coupled cavity structure using Ag and MgF_2 as the metal and dielectric materials, respectively. Ag, with its high average reflectance in the visible range, can function as either a reflecting mirror or an absorbing layer depending on its thickness. For the cavity structure, we deposited a 150-nm thick bottom Ag layer to serve as an optical mirror, while the top Ag layer was deposited thinly to absorb and tunnel incident light into the cavity, resulting in enhanced structural coloration [32]. In addition, we selected MgF_2 as an intermediate layer of the cavity. Fluoride-based compounds, such as MgF_2, can be deposited using a thermal evaporator due to their low vaporization points. However, alternative dielectric materials, such as SiO_2 or TiO_2, could be used and the resonance condition adjusted based on the refraction index of the material.

Fig. 2(a) illustrates the specific fabrication process of the metal grating-coupled MDM cavity structure. Fig. 2(b) shows the corresponding scanning electron Microscopy (SEM) and atomic force microscopy (AFM) images of the fabricated grating pattern. The multilayer cavity structure, which consists of Ag 150 nm, MgF_2 165 nm, Ag 20 nm, and MgF_2 20 nm on a Si substrate in that order, was fabricated using the same thermal evaporator. Notably, a 20-nm thick MgF_2 layer was included to promote the adhesion of the Ag grating. Then, we applied a photoresist (NR9-250PY) by spin-coating onto the cavity. Grating patterns with various pitches were obtained using laser interference lithography (LIL) and their fill factor defined as the width-to-pitch ratio was 0.5. After the development process, residual photoresist was removed using O_2 plasma etching. Finally, a lift-off process was used to fabricate the final structure after an Ag film with a thickness of 20 nm was deposited.

2.3. Optical characteristics of 1D Ag grating coupled Ag/MgF_2/Ag cavity

The measured polarization-resolved reflectance spectra of the 1D Ag grating-coupled Ag/MgF_2/Ag cavities with different pitch values (P = 400, 570, and 800 nm) were obtained at a variety of angles (Fig. 3(a–c)). The dashed lines indicate the wavelength shift of the same cavity modes with increasing angle. The colors of the 1D Ag grating-coupled Ag/MgF_2/Ag cavities with different pitch values, derived from their measured reflection spectra, are summarized in Fig. 3(d). Notably, SPP modes, which were observed exclusively in the p-polarization, redshifted as the angle increased. This behavior is well explained by the momentum matching condition of SPP excitation by a metal grating [30]: $k_{SPP}(\omega) + k_0(\omega)sin(\theta) = m(\frac{2\pi}{P})$ where k_{SPP} is the wave vector of a SPP mode at a metal/dielectric interface, k_0 is the wave vector of the incident light, θ is the angle of incidence, P is the pitch of the metal grating, and m is a mode number. Owing to the distinct mode characteristics, the colors produced by these hierarchically designed optical structures relied on both polarization and angle.

We also conducted RCWA simulations and plotted the photonic band dispersions (i.e., angle-resolved reflectance spectra) for p- and s-polarizations (Fig. 3(e–g)). The simulated results exhibited the same features as the measured data. The monotonically tuned cavity-induced photonic bands solely appeared in the s-polarized spectra. In contrast, the p-polarized spectra exhibited discrete SPP-induced photonic bands in addition to the cavity-induced ones. As the grating pitch increased, the p-polarized spectra became less intricate, resulting from a weak coupling strength between the cavity and SPP modes.

We observed the actual structural color images using a P = 400 nm sample, which exhibited the most striking color variations depending on both polarization and angle. To investigate the full extent of this phenomenon, we employed a rotation stage to alter the angle and a polarizer to obtain polarization-resolved sample images (Fig. 4(a)). By illuminating the sample with a 6700 K light source, we were able to capture vivid structural color images (Fig. 4(b)). For comparison, predicted colors were obtained using the measured spectra of the sample (Fig. 3(a)), as indicated by the colored boxes in the upper right corner of each image. The fabricated sample showed distinct and consistent color changes based on polarization and angle, a result that is in full agreement with our findings in Fig. 3.

2.4. Analysis of photonic band dispersions

We focused on exploring the photonic band dispersions of three different structures: a 1D Ag grating, Ag/MgF_2/Ag cavity, and 1D Ag grating-coupled Ag/MgF_2/Ag cavity (Fig. 5(a)). By simulating their photonic band dispersions for normal incidence and varying the pitch of

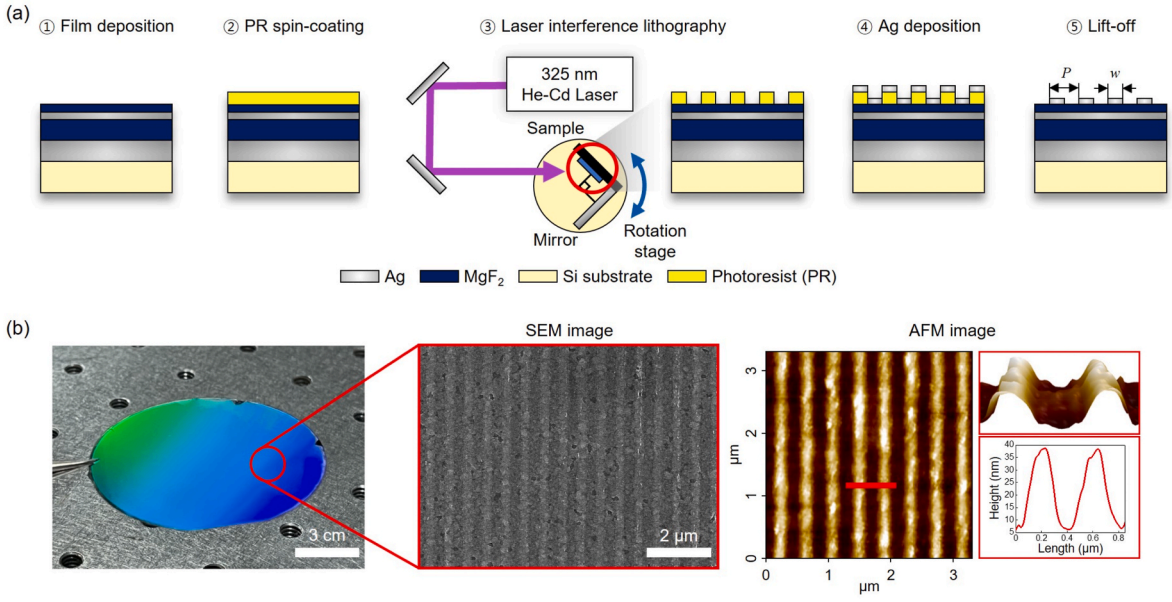

Fig. 2. (a) Schematics illustrating the fabrication process of a 1D Ag grating coupled Ag/MgF_2/Ag cavity. Laser inference lithography (LIL) with a He–Cd laser (325 nm) is used to produce 1D periodic patterns for Ag gratings. (b) Camera, SEM, and AFM image of a LIL-generated 1D pattern with P = 400 nm.

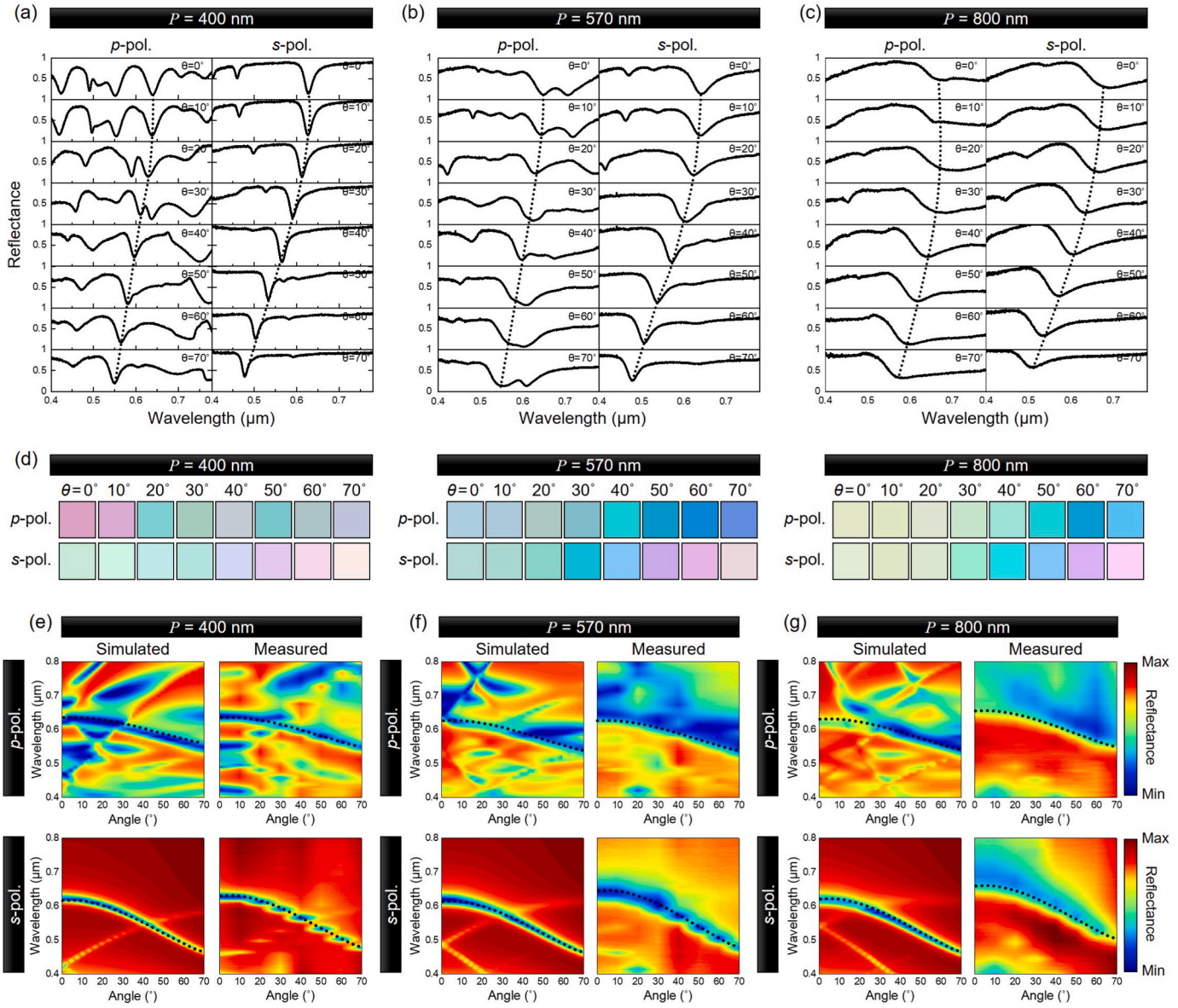

Fig. 3. (a–c) Measured polarization-resolved reflectance spectra of fabricated 1D Ag grating-coupled Ag/MgF_2/Ag cavities with (a) $P = 400$, (b) 570, and (c) 800 nm. The dashed lines indicate the wavelength shift of the same cavity modes. (d) Color tables determined by the measured spectra of the corresponding samples. (e–g) Simulated and measured polarization-resolved photonic band dispersions of the same structures. (For interpretation of the references to color in this figure legend, the reader is referred to the Web version of this article.)

the Ag grating, we were able to gain a deeper understanding of how each mode characteristic affects structural coloration. Our findings revealed that the SPP mode only emerged in the *p*-polarization and redshifted with increasing pitch, while the cavity mode was anchored at a wavelength of 620 nm in both the *p*- and *s*-polarizations. The 1D Ag grating-coupled Ag/MgF_2/Ag cavity was characterized by sustaining multiple SPP-induced photonic bands in the *p*-polarization, setting it apart from the simple 1D Ag grating. Furthermore, mode anticrossing features were clearly observed, as the cavity- and SPP-induced photonic bands were spectrally overlapped. The photonic bands were disconnected near every anticrossing point, with reflectance values rather locally "maximized" at the exact anticrossing point [29,30].

Our study sheds light on the well-known phenomenon of mode anticrossing, which takes place when two or more independent modes reside in the same energy-momentum space, leading to closely split energy levels. The specific condition in which mode anticrossing occurs can be interpreted by the Hamiltonian equation as follows [30]: $H\psi = \begin{pmatrix} E_{cavity} & g \\ g & E_{SPP} \end{pmatrix} \begin{pmatrix} \psi_{cavity} \\ \psi_{SPP} \end{pmatrix} = E \begin{pmatrix} \psi_{cavity} \\ \psi_{SPP} \end{pmatrix}$ where E_{cavity} and E_{SPP} are the energy terms of the cavity and SPP modes, ψ_{cavity} and ψ_{SPP} are the eigenstates of the cavity and plasmon, and g is the coupling strength. For the hierarchical structures studied herein, the coefficient g in the off-diagonal elements is dictated by the thickness of the top Ag layer of the Ag/MgF_2/Ag cavity. In our designed structures, the thickness of the top Ag layer was fixed at 20 nm. If the Ag thickness is too thick, the interaction between the 1D Ag grating and Ag/MgF_2/Ag cavity is marginal, therefore $g = 0$ [32]. This implies that the eigenmodes of the cavity and SPP are uncoupled. Hence, the thickness of the top Ag layer in the MDM cavity should be below a skin depth (i.e., approximately 20 nm for Ag) to induce substantial mode coupling. Notably, the mode coupling results in mode anticrossing. Near every anticrossing point, the *p*-polarized photonic bands are disconnected with reflectance values locally maximized (the bottom panel of Fig. 5(a)). This phenomenon makes the color variation of the hierarchical structures more

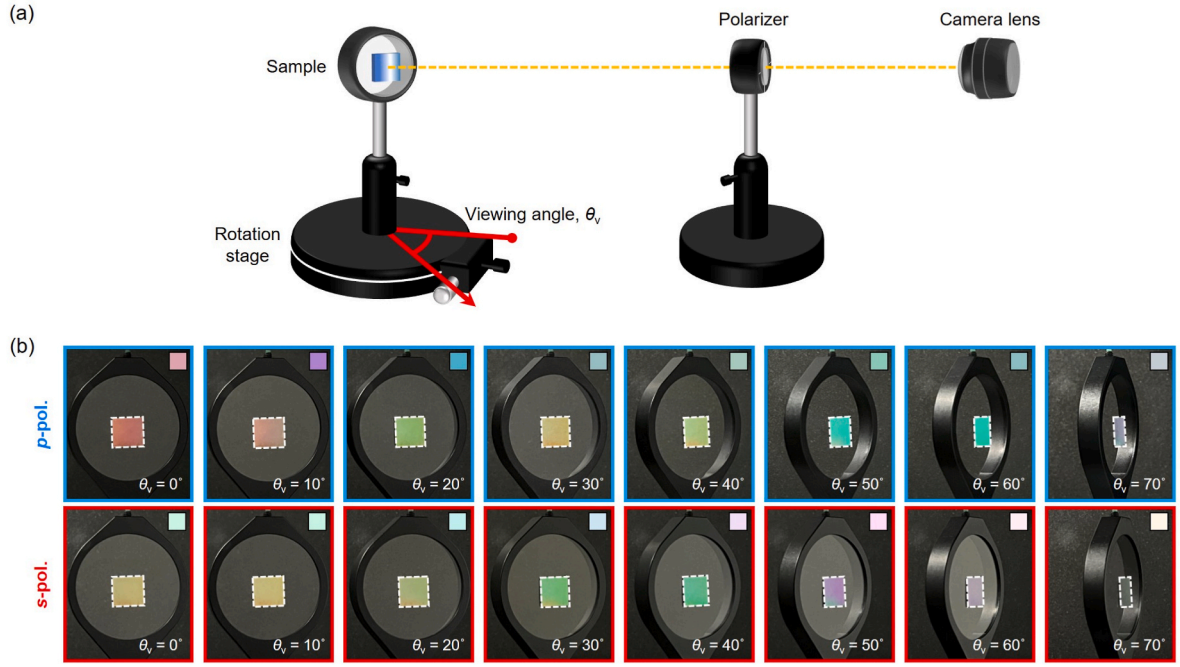

Fig. 4. (a) Schematic of a camera imaging setup. (b) Camera images of the fabricated sample with $P = 400$ nm in Fig. 3a, obtained at a variety of viewing angles in the *p*- and *s*-polarizations. The colored boxes in the upper right corner of each image represent colors determined by the measured spectra of the corresponding samples. (For interpretation of the references to color in this figure legend, the reader is referred to the Web version of this article.)

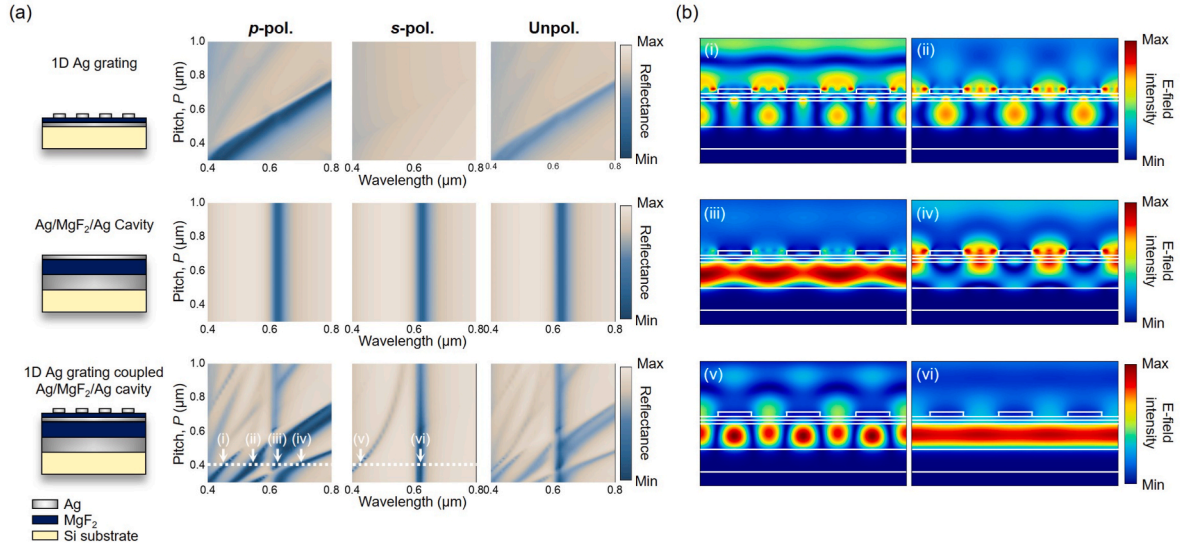

Fig. 5. (a) Simulated pitch–wavelength reflectance dispersions for a 1D Ag grating (top), Ag/MgF_2/Ag cavity (middle), and 1D Ag grating-coupled Ag/MgF_2/Ag cavity (bottom) for *p*-, *s*-, and unpolarized light. (b) Simulated electric-field intensity distributions of the 1D Ag grating-coupled Ag/MgF_2/Ag cavity ($P = 400$ nm), acquired at the wavelengths marked by the arrows in (a) in the *p*- (i–iv) and *s*-polarizations (v and vi).

complicated. With a grating pitch of 400 nm, multiple, pronounced plasmonic modes emerge in the *p*-polarization, making the structural coloration intricate, as demonstrated in Fig. 3(d).

Finally, we performed photonic band dispersion simulations for a 1D Ag grating (top), Ag/MgF_2/Ag cavity (middle), and hierarchically designed 1D Ag grating-coupled Ag/MgF_2/Ag cavity (bottom) for normally incident ($\theta = 0°$) *p*-, *s*-, and unpolarized light (Fig. 5(a)). In the *p*-polarization, the 1D Ag grating exhibited a monotonic, pitch-dependent SPP mode characteristic, whereas its *s*-polarized photonic band dispersion was featureless. The Ag/MgF_2/Ag cavity sustained the same Fabry–Perot mode in both polarizations. In contrast, the hierarchically designed structure yielded intricate photonic band dispersions distinct to polarization. A pitch-dependent photonic band was additionally excited in the *s*-polarization, and multiple vein-like photonic bands were created in the *p*-polarization.

To gain a comprehensive understanding of the structural coloration mechanism, we performed a detailed analysis of the optical modes in a hierarchical structure with a pitch of 400 nm, wherein the *p*-polarized photonic bands appeared intensely. In Fig. 5(a), the wavelengths at which the electric-field intensity distributions were obtained are marked by arrows, and the resulting *p*- and *s*-polarized modes are depicted in Fig. 5(b). In general, when a metal grating is employed, gap plasmon resonances are typically excited, and their energy is confined inside a dielectric interspace between the metal elements [33,34]. Furthermore,

when a waveguide structure is coupled to a metal grating with an appropriate pitch, guided mode resonances can be observed. In the hierarchical structure, the gap plasmon and guided mode resonances were hybridized in the *p*-polarization and identified as modes (i) and (ii). For both modes (i) and (ii), the electric-field intensity was localized in the air gap between the Ag grating elements (identified as gap plasmon resonances) and inside the MgF_2 layer of the MDM cavity (identified as guided mode resonances). The only difference between modes (i) and (ii) is their parity, as the antinodes of their guided mode resonances were alternately positioned. Mode (iii) corresponded to a MDM cavity mode resonance coupled to the gap plasmon resonance. The additional hybrid mode labelled (iv) originated from the SPP resonance localized at the MgF_2/Ag interface of the MDM cavity coupled to the gap plasmon resonance. In contrast, in the *s*-polarization, modes (v) and (vi) arose from guided mode and MDM cavity mode resonances without hybridization, respectively. Therefore, the angular dispersion of the MDM cavity mode resonance was slightly different in the *p*- and *s*-polarizations, as evident from the black dotted curves in Fig. 3(e). We note that the hybridized plasmonic and MDM cavity mode resonances behave distinctly at different incident angles. Overall, the former redshifted with increasing angle only in the *p*-polarization, whereas the latter blueshifted with increasing angle in both polarizations (Fig. 3(e)). The electric field profiles of these modes reveal their unique characteristics, which are crucial in understanding and manipulating the structural coloration produced by the hierarchically designed structure.

3. Conclusions

The optical phenomenon of structural coloration has been investigated through the design and fabrication of a 1D metal grating-coupled MDM cavity capable of switching colors depending on polarization and angle. The combination of the Ag/MgF_2/Ag cavity and 1D Ag grating structures allowed for the observation of multidimensional structural coloration, resulting in a wide range of color variations. By exploring the photonic band dispersions of the fabricated structures, we found that the diverse SPP modes only emerged in the *p*-polarization and redshifted with increasing angle, while the cavity mode blueshifted with increasing angle in both *p*- and *s*-polarizations. We believe that this study will contribute to the fundamental understanding of structural coloration and demonstrate the potential for the development of future optical devices and applications such as anti-counterfeiting technology [3,15,16], optical data storage [14], and holographic display [12,13].

Declaration of competing interest

The authors declare that they have no known competing financial interests or personal relationships that could have appeared to influence the work reported in this paper.

Acknowledgements

This work was supported by the National Research Foundation of Korea through the Basic Science Research Program (RS-2023-00207966) and the Nano Material Technology Development Program (2021M3H4A3A01055870), and by the Basic Research Project (Grant No. 401C2905) funded by Korea Electronics Technology Institute.

References

[1] Y.G. Kim, Y.J. Quan, M.S. Kim, Y. Cho, S.H. Ahn, Lithography-free and highly angle sensitive structural coloration using Fabry–Perot resonance of Tin, ISSN International Centre 8 (2021) 997–1006.
[2] J. Zhao, M. Qiu, X. Yu, X. Yang, W. Jin, D. Lei, Y. Yu, Defining deep-subwavelength-resolution, wide-color-gamut, and large-viewing-angle Flexible subtractive colors with an ultrathin asymmetric Fabry–Perot lossy cavity, Adv. Opt. Mater. 7 (23) (2019) 1600646–1600653.
[3] Y. Jung, H. Jung, H. Choi, H. Lee, Polarization selective color filter based on plasmonic nanograting embedded etalon structures, Nano Lett. 20 (9) (2020) 6344–6350.
[4] Z. Xuan, J. Li, Q. Liu, F. Yi, S. Wang, W. Lu, Artificial structural colors and applications, Innovation 2 (1) (2021) 100081–100095.
[5] L. Cao, P. Fan, E.S. Barnard, A.M. Brown, M.L. Brongersma, Tuning the color of silicon nanostructures, Nano Lett. 10 (7) (2010) 2649–2654.
[6] P. Mao, C. Liu, F. Song, M. Han, S.A. Maier, S. Zhang, Manipulating disordered plasmonic systems by external cavity with transition from broadband absorption to reconfigurable reflection, Nat. Commun. 11 (1) (2020) 1538–1544.
[7] B. Zeng, Y. Gao, F.J. Bartoli, Ultrathin nanostructured metals for highly transmissive plasmonic subtractive color filters, Sci. Rep. 3 (1) (2013) 2840–2848.
[8] I. Koirala, V.R. Shrestha, C.S. Park, S.S. Lee, D.Y. Choi, Polarization-controlled broad color palette based on an ultrathin one-dimensional resonant grating structure, Sci. Rep. 7 (1) (2017), 40073.
[9] Z. Li, S. Butun, K. Aydin, Large-area, Lithography-free super absorbers and color filters at visible frequencies using ultrathin metallic films, ACS Photonics 2 (2) (2015) 183–188.
[10] J.C. Blake, S. Rossi, M.P. Jonsson, A. Dahlin, Scalable reflective plasmonic structural colors from nanoparticles and cavity resonances – the Cyan-magenta-yellow approach, Adv. Opt. Mater. 10 (13) (2022), 2200471.
[11] J.G. Park, S.H. Kim, S. Magkiriadou, T.M. Choi, Y.S. Kim, V.N. Manoharan, Full-spectrum photonic pigments with non-iridescent structural colors through colloidal assembly, Angew. Chem., Int. Ed. Engl. 53 (11) (2014) 2899–2903.
[12] J. Li, Y. Chen, Y. Hu, H. Duan, N. Liu, Magnesium-based metasurfaces for dual-function switching between dynamic holography and dynamic color display, ACS Nano 14 (7) (2020) 7892–7898.
[13] R. Zhao, L. Huang, Y. Wang, Recent advances in multi-dimensional metasurfaces holographic technologies, PhotoniX 1 (20) (2020) 1–24.
[14] M. Rezaei, H. Jiang, R. Qarehbaghi, M. Naghshineh, B. Kaminska, Rapid production of structural color images with optical data storage capabilities, SPIE 9374 (2015), 93740O.
[15] D. Yang, G. Liao, S. Huang, Hand painting of noniridescent structural multicolor through the self-assembly of YOHCO3 colloids and its application for anti-counterfeiting, Langmuir 35 (25) (2019) 8428–8435.
[16] Z. Gao, C. Huang, D. Yang, H. Zhang, J. Guo, J. Wei, Dual-mode multicolored photonic crystal patterns enabled by ultraviolet-responsive core-shell colloidal spheres, Dyes Pigments 148 (2018) 108–117.
[17] C. Ji, K.T. Lee, T. Xu, J. Zhou, H.J. Park, L.J. Guo, Engineering light at the nanoscale: structural color filters and broadband perfect absorbers, Adv. Opt. Mater. 5 (20) (2017) 1700368–1700389.
[18] Y. Chen, Z. Dong, Y. Zhou, J. Tao, W. Tong, Y. Wu, W. Liu, B. Wang, X. Dai, X. Wang, Wavelength modulation characteristics of metal gratings on Si-based blocked-impurity-band (BIB) Terahertz detectors, Micromachines 13 (5) (2022) 811–818.
[19] S.M. Cho, S.H. Cheon, T.Y. Kim, C.S. Ah, J. Song, H. Ryu, H.Y. Chu, Design and fabrication of integrated Fabry-Perot type color reflector for reflective displays, J. Nanosci. Nanotechnol. 16 (5) (2016) 5038–5043.
[20] Z. Yang, Y. Zhou, Y. Chen, Y. Wang, P. Dai, Z. Zhang, H. Duan, Reflective color filters and monolithic color printing based on asymmetric Fabry–Perot cavities using nickel as a broadband absorber, Adv. Opt. Mater. 4 (8) (2016) 1196–1202.
[21] F. Liu, H. Shi, X. Zhu, P. Dai, Z. Lin, Y. Long, Z. Xie, Y. Zhou, H. Duan, Tunable reflective color filters based on asymmetric Fabry–Perot cavities employing ultrathin Ge 2 Sb 2 Te5 as a broadband absorber, Appl. Opt. 57 (30) (2018) 9040–9045.
[22] K.T. Lee, S.Y. Han, Z. Li, H.W. Baac, H.J. Park, Flexible high-color-purity structural color filters based on a higher-order optical resonance suppression, Sci. Rep. 9 (1) (2019), 14917.
[23] F. Chen, Y. Huang, R. Li, S. Zhang, B. Wang, W. Zhang, X. Wu, Q. Jiang, F. Wang, R. Zhang, Bio-inspired structural colors and their applications, Chem. Commun. 57 (99) (2021) 13448–13464.
[24] J.B. Kim, S.Y. Lee, J.M. Lee, S.H. Kim, Designing structural-color patterns composed of colloidal arrays, ACS Appl. Mater. Interfaces 11 (16) (2019) 14485–14509.
[25] H.S. Lee, T.S. Shim, H. Hwang, S.M. Yang, S.H. Kim, Colloidal photonic crystals toward structural color palettes for security materials, Chem. Mater. 25 (13) (2013) 2684–2690.
[26] J. Zhu, N. Li, MIM waveguide structure consisting of a semicircular resonant cavity coupled with a key-shaped resonant cavity, Opt Express 28 (14) (2020) 19978–19987.
[27] R.H. Ritchie, E.T. Arakawa, J.J. Cowan, R.N. Hamm, Surface-plasmon resonance effect in grating diffraction, Phys. Rev. Lett. 21 (22) (1968) 1530–1533.
[28] H.S. Lee, Y.T. Yoon, S.S. Lee, S.H. Kim, K.D. Lee, Color filter based on a subwavelength patterned metal grating, Opt Express 15 (23) (2007) 15457–15463.
[29] R. Ameling, H. Giessen, Microcavity plasmonics: strong coupling of photonic cavities and plasmons, Laser Photon. Rev. 7 (2) (2013) 141–169.
[30] S. Chen, G. Li, D. Lei, K.W. Cheah, Efficient energy exchange between plasmon and cavity modes via Rabi-analogue splitting in a hybrid plasmonic nanocavity, Nanoscale 5 (19) (2013) 9129–9133.
[31] M.J. Preiner, K.T. Shimizu, J.S. White, N.A. Melosh, Efficient optical coupling into metal-insulator-metal plasmon modes with subwavelength diffraction gratings, Appl. Phys. Lett. 92 (11) (2008), 113109.

[32] M. ElKabbash, T. Letsou, S.A. Jalil, N. Hoffman, J. Zhang, J. Rutledge, A. R. Lininger, C.H. Fann, M. Hinczewski, G. Strangi, C. Guo, Fano-resonant ultrathin film optical coatings, Nat. Nanotechnol. 16 (4) (2021) 440–446.
[33] J.-W. Cho, S.J. Park, S.J. Park, Y.B. Kim, Y.J. Moon, S.-K. Kim, Cooling metals via gap plasmon resonance, Nano Lett. 21 (9) (2021) 3974–3980.
[34] D.-W. Hwang, J.-W. Cho, S.-K. Kim, Spectral tuning of plasmonic absorption for high-transmittance nanostructured metal electrodes, J. Kor. Phys. Soc. 73 (5) (2018) 567–573.